

Auger rates for highly charged ions near an insulator surface

Joachim Burgdörfer,¹ Carlos O. Reinhold,² and Fred Meyer²

¹*Institute for Theoretical Physics, Vienna University of Technology,*

Wiedner Hauptstr. 8-10/136, A-1040 Vienna, Austria

²*Physics Division, Oak Ridge National Laboratory, Oak Ridge, TN 37831-6372, USA*

(Dated: August 29, 2002)

Abstract

We present estimates for two-electron transition rates for highly charged ions interacting with a LiF surface. Three different processes are considered: intra-atomic Auger, Auger capture and Auger deexcitation. They represent input for simulations of neutralization of HCI's near surfaces. Simple universal estimates as functions of the distance to the surface, as well as initial and final state populations are presented which are believed to provide reasonable order of magnitude estimates.

PACS numbers: 34.50.Dy, 34.70.+e, 79.20.Rf

I. INTRODUCTION

Since the pioneering work on ion – surface interactions by Hagstrum [1], it has been appreciated that two-electron processes represent alternative channels to resonant (one-electron) transfer for neutralization of ions approaching solid surfaces. In particular, when resonant transfer is suppressed due to an energy mismatch between the occupied levels in the solid and unoccupied levels in the ion, two-electron processes are expected to provide important, potentially even dominant contributions. For highly charged ion (HCI)-surface interactions, which have recently become the focus of a large number of investigations [2–8], the density of projectile states is sufficiently high to preclude blocking effects for resonant transfer. Nevertheless, a satisfactory simulation of the entire neutralization sequence requires two-electron Auger transition rates as input [4, 9, 10]. A theoretical description of two-electron transition rates remains a challenge. Even in the simplest case of intra-atomic Auger processes (Fig. 1a), ab-initio calculations beyond the Hartree-Fock (HF) approximation level are difficult, in particular far from the ground state with many open shells present. HF calculations are expected, however, to provide reasonable estimates (within a factor 2 or so) for configuration – averaged rates. Much less is known about rates for Auger capture (AC) or Auger deexcitations (AD) (Figs. 1b and 1c). For simple metals for which a jellium description is applicable, considerable progress has been made [11, 12]. However, for insulator surfaces such as LiF or other alkali - halide surfaces, for which many of the simplifying assumptions underlying a jellium model such as translational invariance along the surface break down, no quantitative treatment of these Auger processes is available to our knowledge. Even order-of-magnitude estimates appear to be lacking. The aim of this communication is to provide such estimates, which are presently being used in a simulation for the neutralization sequence of HCI's in front of an LiF surface [13]. The focus is therefore on the dominant, i.e. fastest, Auger rates that may have a non-negligible impact on the overall speed on the neutralization and relaxation process. Our approach to arrive at order-of-magnitude estimates is based on a generalization of simple scaling relations for dominant intra-atomic Auger rates. Atomic units are used throughout unless otherwise indicated.

II. SCALING RELATIONS FOR AUGER RATES

A. Intra-atomic Auger rates

We begin by briefly recalling a simple fundamental scaling relation we have found previously for intra-atomic Auger processes. Focusing on the first allowed dominant Auger decay of two s electrons in an upper shell n decaying into an empty lower shell n' , it was found that the transition rate can be fitted with considerable accuracy to the functional form [4]

$$\Gamma_{AI}(ns^2 \rightarrow n's) = \frac{5.06 \times 10^{-3} \text{ a.u.}}{(n - n')^{3.46}} = \frac{2.1 \times 10^{14} \text{ sec}^{-1}}{(n - n')^{3.46}}. \quad (1)$$

This relationship was deduced from calculations of Auger rates for isolated atoms in the gas phase using the Cowan code [14]. This expression features several remarkable aspects: Most notably, it is valid for all pairs of n and n' levels corresponding to the first energetically allowed transition and it is independent of the nuclear charge of the ion. Fig. 2a illustrates the validity of Eq. (1) for transitions from a given n to the highest n' consistent with the above-ionization-threshold energy of the second ionized electron. This transition is, in general, the fastest decay channel from the initial n level. Moreover, and more surprisingly, Fig. 2b shows that (1) can be even used as an estimate for Auger transitions to energy levels n' lower than that giving the first allowed transition. In simulations of the neutralization sequence [4, 10, 13], however, the latter do not play an important role, since the relaxation of the ion proceeds mostly as a sequence of the fastest processes.

The applicability of Eq. (1) can be extended considerably. For a many-electron atom (or ion), the intra-atomic Auger rates can be calculated when one considers Eq. (1) as a two-body ‘‘collision kernel’’ for electron - electron scattering and accounts for multiplicities of initial single-particles states and Pauli blocking for final states in analogy to a quantum Boltzmann collision term. Specifically, when the total electronic energies of the projectile ion in its initial and final configurations are $E_i^P(D) > E_f^P(D)$, the Auger decay $n \rightarrow n'$ is allowed and its rates is given by

$$\Gamma^{AI}(D, n \rightarrow n') = M^{AI}(P_n) B^{AI}(P_{n'}) \Gamma_{AI}(ns^2 \rightarrow n's^2), \quad (2)$$

where M^{AI} and B^{AI} are the multiplicity and blocking factors for initial and final states with populations $P_n, P_{n'}$ of the n and n' shells respectively. As the condition for the total

energies $E_{i,f}^P$ is dependent on the distance D from the surface, Eq. (2) contains modifications of the atomic Auger rates due to the interaction with the surface and is, thus, implicitly D -dependent. Thereby, the distortion of the electronic structure due to the coupling between the projectile ion and the surface can be taken into account. The initial state multiplicity factor $M^{AI}(P_n)$ for electrons in the same shell is well approximated (Fig. 3a) by the standard binomial expression [6],

$$M^{AI}(P_n) = \frac{(P_n - 1) P_n}{2}, \quad (3)$$

where we have also shown for comparison the choice $M^{AI} = P_n/2$, which has been obtained from calculations of Auger rates in the bulk of metals [16]. Obviously, Eq. (3) appears better suited for atomic Auger transitions above the surface. In the special case of transitions from the L to the K shell, the $2s$ and the $2p$ subshells should be considered as non-equivalent, since dominant monopole transitions ($\ell \rightarrow \ell$) are blocked for $2p$ electrons. In this case, the multiplicity factor should be replaced by

$$M^{AI}(P_2) = \frac{1}{2} [P_{2s}(P_{2s} - 1) + \beta P_{2s}P_{2p}], \quad (4)$$

with β of the order of one, as displayed in Fig. 3b. We note that such a decomposition into subshells is outside the scope of current simulations [13] and is not required for all higher shells and, hence, for the relaxation sequence of HCI's.

Fig. 4 displays the comparison of the numerically determined blocking factors with the standard Pauli blocking factor of a quantum Boltzmann collision term, $(1 - P_n/2n'^2)$ in terms of the number of available unoccupied final states. We find that a more appropriate choice is

$$B^{AI}(P_{n'}) = \left(1 - \frac{P_{n'}}{2n'^2}\right)^2, \quad (5)$$

i.e. with the square of the Pauli blocking factor. The additional factor $(1 - P_n/2n'^2)$ in Eq. (5), whose origin is not Pauli blocking, can be qualitatively understood in terms of the reduction of orbital overlap and of available phase space of the emitted electron when the population ($P_{n'}$) enhances the screening in the final shell n' .

The point to be noted is that such a decomposition/separation/factoring for such a characteristic time scale of the Auger transition rates emerges from the self-consistent HF calculation only when initial and final orbitals are orthogonal to each other and spurious overlap contributions are eliminated. The latter has been found to have a strong influence on effective rates [11]. The fact that a large body of Hartree-Fock data for intra-atomic Auger rates

can be reduced to such a simple Z -independent “universal” transition rate, which depends on the number of electrons only in terms of multiplicity and blocking factors, suggests that the description of Auger rates in terms of this “universal” inelastic two-body scattering rate for electrons of atomic density should be extendable to more complex Auger processes. It is therefore tempting to employ the same “collision kernel” for the determination of Auger capture and Auger deexcitation rates near surfaces, for which self-consistent calculations including orthogonalization of all relevant orbitals are difficult to achieve.

B. Auger deexcitation and Auger capture

In contrast to Auger rates near metal surfaces (e.g. [1, 11]), very little information is available for insulators and estimates for inter-atomic Auger rates applicable in the vicinity of insulator surfaces have remained elusive. We therefore attempt to provide such estimates based on a generalization of the inelastic electron-electron scattering rate (Eq. (1) and (2)). For simulations of neutralization of HCl’s, use of such simple rates is necessary, since generation of data sets for all states, all configurations, as well as all relative positions between the HCl, at \vec{R} , and the lattice vector \vec{a} , $\vec{a} = (i, j, k) d$ is not feasible and microscopic ab-initio calculations in cases where the jellium approximation is not applicable present fundamental difficulties. Therefore, drastic simplifications are called for.

Even though the following reasoning is general, we focus here on LiF surfaces ($d = 3.8 \text{ a.u.}$), for which the active electrons involved in the inter-atomic Auger processes are the $2p$ electrons localized near the F^- sites at the surface and we use $P_{\vec{a}}^{(F)}$ to denote the electronic population of the surface fluorine ion at the lattice site \vec{a} ($P_{\vec{a}}^{(F)} = 6$ for an isolated surface). Our point of departure is that for small distances from the surface, i.e. small distances $D_{\vec{a}} = |\vec{R} - \vec{a}|$ between the projectile and the F^- sites in the surface, inter-atomic Auger rates should closely resemble Auger results for a transient quasi-molecule [17] formed by the projectile and the surface atom. The latter are, in turn, closely related to intra-atomic rates discussed above. In fact, when the distance between the ion and the active site, $D_{\vec{a}} = |\vec{R} - \vec{a}|$, is small, electrons in the molecules are “shared”, and inter-atomic and intra-atomic Auger rates become nearly indistinguishable from each other. Molecular sharing sets in when the potential surface of the combined system of HCl and surface atom allows for over-barrier (or more generally, near-barrier tunneling) transitions of an electron between the potential

wells of the surface atom and the HCl. In other words, the effective electron density of the surface extends further out into the vacuum due to the Coulomb field of the HCl than for an unperturbed surface. This effect has turned out to be important for jellium surfaces [11] and can be taken into account within classical simulations for insulators. Accordingly, for distances smaller than the sharing distance, D_S , we adopt the following forms for the effective rate for Auger capture (AC) and for Auger deexcitation (AD)

$$\Gamma^{AC} (D_{\bar{a}} \leq D_S, \bar{a}^{(F)} \rightarrow n') = M^{AC}(P_{\bar{a}}^{(F)}) B^{AI}(P_{n'}) \Gamma^{AI}(ns^2 \rightarrow n's) \quad (6)$$

$$\Gamma^{AD} (D_{\bar{a}} \leq D_S, [\bar{a}^{(F)}, n] \rightarrow n') = M^{AD}(P_n, P_{\bar{a}}^{(F)}) B^{AI}(P_{n'}) \Gamma^{AI}(ns^2 \rightarrow n's) \quad , \quad (7)$$

with multiplicity factors corresponding to the number of pairs of electrons available in the initial configuration

$$M^{AD} = P_n P_{\bar{a}}^{(F)} \quad (8)$$

$$M^{AC} = \frac{1}{2} P_{\bar{a}}^{(F)} (P_{\bar{a}}^{(F)} - 1) \quad , \quad (9)$$

where $P_{\bar{a}}^{(F)}$ denotes the population of the surface fluorine atom at the lattice site \bar{a} . The effective sharing distance can be calculated from a classical trajectory Monte Carlo (CTMC) simulation of the electronic dynamics at fixed inter-nuclear distance. It could be augmented by below-barrier tunneling Monte Carlo calculations [18].

To extend Eq. (6) and (7) to distances $D_{\bar{a}} > D_S$ we incorporate the large-distance behavior of the inter-atomic Auger rates observed for metals [11] and molecules [19]. The Auger deexcitation rates should decrease as $D_{\bar{a}}^{-3}$ whereas the Auger capture rate should decrease approximately exponentially following the available probability density of target electrons extending out into the vacuum. We therefore extrapolate to larger distances as

$$\Gamma^{AC} (D_{\bar{a}} > D_S) = \frac{\rho(D_{\bar{a}})}{D_{\bar{a}}} \Gamma^{AC} (D_{\bar{a}} = D_S) \quad (10)$$

$$\Gamma^{AD} (D_{\bar{a}} > D_S) = \frac{1}{2} \left[\left(\frac{D_S}{D_{\bar{a}}} \right)^3 + \rho(D_{\bar{a}}) \right] \Gamma^{AD} (D_{\bar{a}} = D_S) \quad (11)$$

where $\rho(D_{\bar{a}}) = \exp[-2\sqrt{-2E_{i0}^F}(D_{\bar{a}} - D_S)]$ (representing the exponential decay of the electronic density) and E_{i0}^F is the orbital energy of a fluorine ion embedded in the crystal. While the smooth transitions of the rates from the molecular ($D_{\bar{a}} < D_S$) to the asymptotic regime

($D_{\bar{a}} \gg D_S$) as implied by Eq. (10) and (11), are certainly an oversimplification, the present functional form should be capable of providing a reasonable order of magnitude estimate.

The $D_{\bar{a}}^{-3}$ dependence of the Auger deexcitation rate at large distances (Eq. 11) can be extracted as follows. Denoting the coordinate of the electron relative to the parent fluorine by \vec{r}_F and of the electron relative to the parent projectile \vec{r}_P , an LCAO expansion of the wavefunction of the initial states of the two active electrons (1 and 2) reads

$$\begin{aligned}\phi_1(\vec{r}_1) &= c_1^P \phi_1^P(\vec{r}_{1P}) + c_1^F \phi_1^F(\vec{r}_{1F}) \\ \phi_2(\vec{r}_2) &= c_2^P \phi_2^P(\vec{r}_{2P}) + c_2^F \phi_2^F(\vec{r}_{2F}) \quad ,\end{aligned}\tag{12}$$

where the atomic expansion coefficients $c_j^{P,F}$ are assumed to be only weakly dependent on $D_{\bar{a}}$ when the atomic (or ionic) states are asymptotically degenerate. For the final state we assume, for simplicity, a simple product form, $\phi_\epsilon^\epsilon(\vec{r}_1)\phi_{2f}^P(\vec{r}_{2P})$ (neglecting exchange for the moment), where the continuum state ϕ_ϵ is delocalized and, in particular, not exponentially localized around the fluorine atom. For the direct part the deexcitation rate we find

$$\begin{aligned}\Gamma &= \left| c_1^P c_2^P \left\langle \phi_1^\epsilon \phi_{2f}^P \left| \frac{1}{r_{12}} \right| \phi_1^P \phi_2^P \right\rangle + c_1^F c_2^P \left\langle \phi_1^\epsilon \phi_{2f}^P \left| \frac{1}{r_{12}} \right| \phi_1^F \phi_2^P \right\rangle \right. \\ &\quad \left. + c_1^P c_2^F \left\langle \phi_1^\epsilon \phi_{2f}^P \left| \frac{1}{r_{12}} \right| \phi_1^P \phi_2^F \right\rangle + c_1^F c_2^F \left\langle \phi_1^\epsilon \phi_{2f}^P \left| \frac{1}{r_{12}} \right| \phi_1^F \phi_2^F \right\rangle \right|^2 ,\end{aligned}\tag{13}$$

where the inter-atomic distance is given by $r_{12} = |\vec{r}_{2P} - \vec{D}_{\bar{a}} - \vec{r}_{1F}|$. The first term in Eq. (13) is of single-center character, and apart from $D_{\bar{a}}$ dependencies of the expansion coefficients (e.g. near avoided crossings), are nearly $D_{\bar{a}}$ independent. The last two terms are of two-center character and decay (approximately) exponentially. The second term in Eq. (13) provides the leading term in the $D_{\bar{a}}$ dependence. A multipole expansion of $1/r_{12}$ up to second order together with the orthogonality relations yields for the second term,

$$\begin{aligned}\left\langle \phi_1^\epsilon \phi_{2f}^P \left| \frac{1}{r_{12}} \right| \phi_1^F \phi_2^P \right\rangle &\simeq \frac{1}{D_{\bar{a}}^3} \left[\langle \phi_1^\epsilon | \vec{r}_{1F} | \phi_1^F \rangle \langle \phi_{2f}^P | \vec{r}_{2P} | \phi_{2f}^P \rangle \right. \\ &\quad \left. - 3 \langle \phi_1^\epsilon | \hat{D}_{\bar{a}} \cdot \vec{r}_{1F} | \phi_1^F \rangle \langle \phi_{2f}^P | \hat{D}_{\bar{a}} \cdot \vec{r}_{2P} | \phi_{2f}^P \rangle \right] ,\end{aligned}\tag{14}$$

Substituting Eq. (14) into Eq. (13) results in an interference between the first and the second term in Eq. (13) with

$$\Gamma^{AD} \underset{D_{\bar{a}} \rightarrow \infty}{\propto} D_{\bar{a}}^{-3} ,\tag{15}$$

as explicitly built into Eq. (11) and also numerically observed in [11]. The exchange contribution from antisymmetrized wavefunctions does not alter Eq. (15). One important conclusion from Eq. (14) is that for Auger deexcitation, dipole - allowed intra-atomic transitions dominate. This prediction is confirmed by numerical results for jellium surfaces [11]. A similar analysis for Auger capture shows that in this case the leading term decays approximately exponentially, as anticipated in Eq. (10).

III. COMPARISON WITH DATA

A direct test of the proposed estimates for intra-atomic Auger rates for HCI-insulator surfaces would be highly desirable but currently difficult to perform due to the lack of any experimental data or ab-initio calculations. Indirect tests are possible through their use in complete simulations of the neutralization sequence and comparison with experimental data for the resulting electron emission and charge distribution. Results of such simulations are forthcoming [13]. The significance of such indirect tests is, however, fairly limited due to the complexity of the neutralization or relaxation process which averages over a large number of competing channels.

Alternative tests can be performed, however, by considering the case of ion – metal interactions, for which data from ab-initio calculations within the framework of jellium approximations are available. Even though the present estimates, based on localized atomic orbitals is not intended for such systems, they nevertheless can be, with caution, applied to the limit of delocalized electrons.

In Fig. 5 we present a comparison between the present approach and calculations [12] of the total Auger rate for filling a single hole in the K shell of an ion immersed in a homogeneous jellium (bulk limit) with $r_s = 2$ as a function of the nuclear charge Z . Note that only the total rate rather than the initial subshell specific rates can be compared since there is no obvious mapping between atomic and jellium subshell states. For low Z only few excited states are bound in jellium. This implies ambiguities as to the initial state multiplicity employed (Eq. (3), (4)). Taking into account that the DFT calculation [12] predicts that only the “ $2s$ ” orbitals are populated for low Z and for $Z > 8$ also $2p$ orbitals contribute, Eqs. (2-4) predict the step function displayed in Fig. 5. The overall agreement of our estimate for almost all Z with the DFT calculation for the Auger rates is

astonishingly good. The case $Z = 2$ (He^+) constitutes a remarkable exception, the origin of which is currently not yet understood. The anomalously high Auger rate found in the DFT calculation for He^+ could, in principle, be reproduced by assuming a high initial state population of a “quasi-bound” $n = 2$ shell of an He^- complex, but there is no compelling reason to do so. These difficulties for low Z ($\simeq 2$) are, however, of no consequence for simulations for highly charged ions.

A second comparison can be made with the D dependence of the Auger rates calculated for ion - jellium interactions [11] (for metals $D_{\bar{a}} \equiv D$ and is given by the distance to the jellium edge). The D dependence of both Auger deexcitation as well as Auger capture (Fig. 6) can be reasonably well fitted by Eqs. (10) and (11) for distances $D > D_S \sim 2.5a.u.$. As the calculation in Ref. [11] refers to He^+ , the same discrepancy is observed for $D < D_S$, as for the comparison with bulk jellium (Fig. 5).

In summary, we have proposed simple estimates for rates for intra-atomic Auger decay, Auger capture and Auger deexcitation in ion – surface interactions which are based on a simple “universal” electron - electron scattering rate as collision kernel for Auger rates in many-electron systems. First comparisons with experimental data for the neutralization of insulator surfaces [13] as well as ab-initio calculations for ions in front of jellium surfaces show surprisingly good overall agreement.

Acknowledgement

This work was supported by the FWF (Austria). COR and FM acknowledge support by the DCS, OBES, USDOE, managed by UT-Battelle, LLC, under contract DE-AC05-00OR22725.

-
- [1] H. D. Hagstrum, *Phys. Rev.* **96**, 336 (1954).
 - [2] A. Arnau, F. Aumayr, P. M. Echenique, M. Grether, W. Heiland, J. Limburg, R. Morgenstern, P. Roncin, S. Schippers, R. Schuch, N. Stolterfoht, P. Varga, T. J. M. Zouros, and HP. Winter, *Surf. Sci. Rep.* **27**, 113 (1997).
 - [3] J. Burgdörfer in *Review of Fundamental Processes and Applications of Atoms and Ions*, C.D. Lin (Ed.), World Scientific, Singapore, 1993.

- [4] J. Burgdörfer, P. Lerner, and F. W. Meyer, *Phys. Rev. A* **44**, 5674 (1991).
- [5] HP. Winter and F. Aumayr, *J. Phys. B: At. Mol. Phys.* **32**, R39 (1999).
- [6] L. Wirtz, C. Lemell, C. O. Reinhold, L. Hägg, and J. Burgdörfer, *Nucl. Instr. Meth. B* **182**, 36 (2001).
- [7] J.-P. Briand, L. de Billy, P. Charles, S. Essabaa, P. Briand, R. Geller, J.-P. Desclaux, S. Bliman, and C. Ristori, *Phys. Rev. Lett.* **65**, 159 (1990).
- [8] F. W. Meyer, V. A. Morozov, J. Mrogenda, C. R. Vane, and S. Datz, *Nucl. Instr. Meth. B* **193**, 508 (2002).
- [9] L. Hägg, C. O. Reinhold, and J. Burgdörfer, *Phys. Rev. A* **55**, 2097 (1997).
- [10] J. Ducrée, F. Casali, and U. Thumm, *Phys. Rev. A* **57**, 338 (1998).
- [11] M.A. Cazadilla, N. Lorente, R. Diez Muino, J.P. Gauyacq, D. Teillet-Billy, and P.M. Echenique, *Phys. Rev. B* **58**, 13991 (1998).
- [12] S. Deutscher, R. Diez Muino, A. Arnau, A. Salin, and E. Zaremba, *Nuc. Instr. Meth. B* **182**, 8 (2001).
- [13] L. Wirtz, C. Reinhold, C. Lemell, and J. Burgdörfer, submitted for publication to *Phys. Rev. A* (2002).
- [14] R. D. Cowan, *The Theory of Atomic Structure and Spectra*, University of California Press, Berkeley, 1981.
- [15] The present rates were calculated using an extension of the Cowan code developed by S. Schippers; S. Schippers, J. Limburg, J. Das, R. Hoekstra, and R. Morgenstern, *Phys. Rev. A* **50**, 540 (1994).
- [16] R. Diez Muino, A. Salin, N. Stoltenfoht, A. Arnau and P. Echenique, *Phys. Rev. A* **57**, 1126 (1998).
- [17] M. Corville and T.D. Thomas, *Phys. Rev. A* **43**, 6053 (1991).
- [18] J. Cohen, *Phys. Rev. A* **64**, 043412 (2001).
- [19] A. Kay, E. Arenholz, S. Mun, F.J. Garcia de Abajo, C.S. Fadley, R. Denecke, Z. Hussain, and M.A. VanHove, *Science* **281**, 679 (1998).

FIGURE CAPTIONS

Figure 1: Auger processes near LiF surfaces: (a) intra-atomic Auger of autoionization (AI) (b) Auger capture from a fluorine (F) atom by a projectile (P) (c) Auger deexcitation (AD).

Figure 2: Intra-atomic Auger transition rates $\Gamma_{AI}(ns^2 \rightarrow n's)$ for $Ne^{8+}(ns^2)$ ions as a function of $\Delta n = n - n'$: (a) first allowed transitions (open squares) and (b) all Auger transitions for $n = 2$ (open squares), $n = 3$ (solid triangles), $n = 4$ (open triangles), $n = 5$ (stars), and $n = 7$ (solid circles).

Figure 3: (a) LMM Auger transition rates for an empty L shell as a function of the number of electrons P_3 in the M shell of a configuration average of the $3s$ and $3p$ orbitals. (b) KLL Auger transition rates for an empty K shell as a function of the number of electrons P_2 in the L shell in the $(2s^2, 2p^{(P_2-2)})$ configuration. The symbols represent the result of Auger calculations using the Cowan code. The lines illustrate the different functional forms indicated in the figures.

Figure 4: LMM Auger transition rates as a function of the population of the L shell, P_2 . The symbols represent the result of Auger calculations using the Cowan code. The solid symbols have been obtained using a $3s^2$ configuration of the M shell and an average configuration with P_2 electrons in the L shell. The open symbols correspond to average configurations of both the upper and lower levels.

Figure 5: Total K shell filling rate of an ion with a single K hole embedded in a jellium ($r_s = 2$) as a function of the nuclear charge. The symbols connected by a dashed line represent the DFT calculation of Ref. [12]. The horizontal solid lines correspond to the intra-atomic Auger rates for the $(1s^1, 2s^2, 2p^0)$ and $(1s^1, 2s^2, 2p^6)$ configurations. The vertical lines indicate the nuclear charge at which the $2s$ and $2p$ orbitals can exist inside the solid as bound states.

Figure 6: Auger capture (AC) and Auger deexcitation (AD) rates as for a He^+ ion in front of a jellium surface ($r_s = 2$) as a function of the distance to the jellium edge, D . The symbols connected by a dashed line represent the DFT calculations of Refs. [12] and [11] assuming that the image plane lies at 0.7a.u. above the jellium edge. The solid lines were calculated

using Eqs. (10) and (11) with the replacement $D_{\tilde{a}} = D$, $D_S = 2.5a.u.$, and $E_{0i}^F = \phi = 4.1eV$ (workfunction of Aluminum).

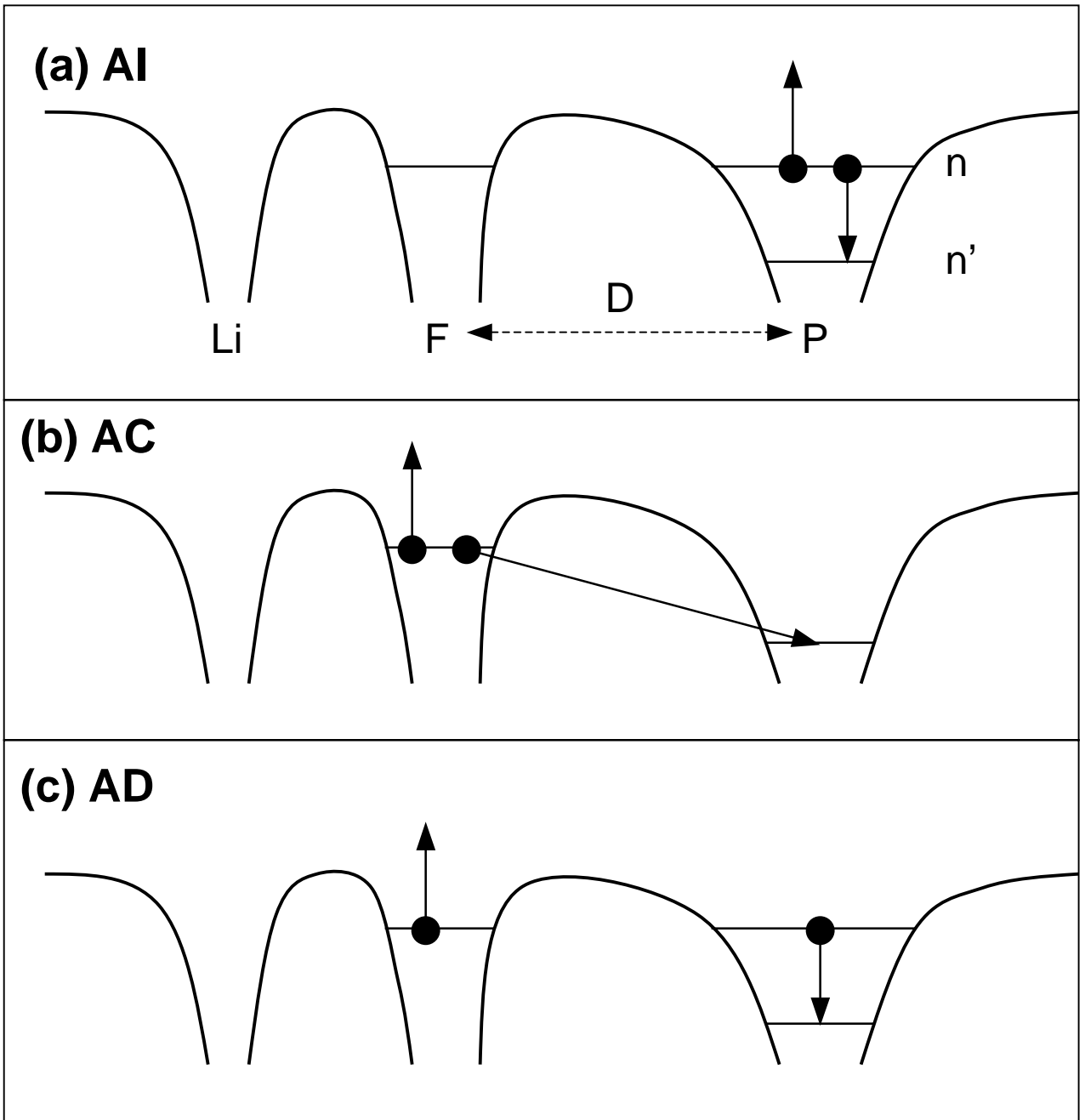


Figure 1

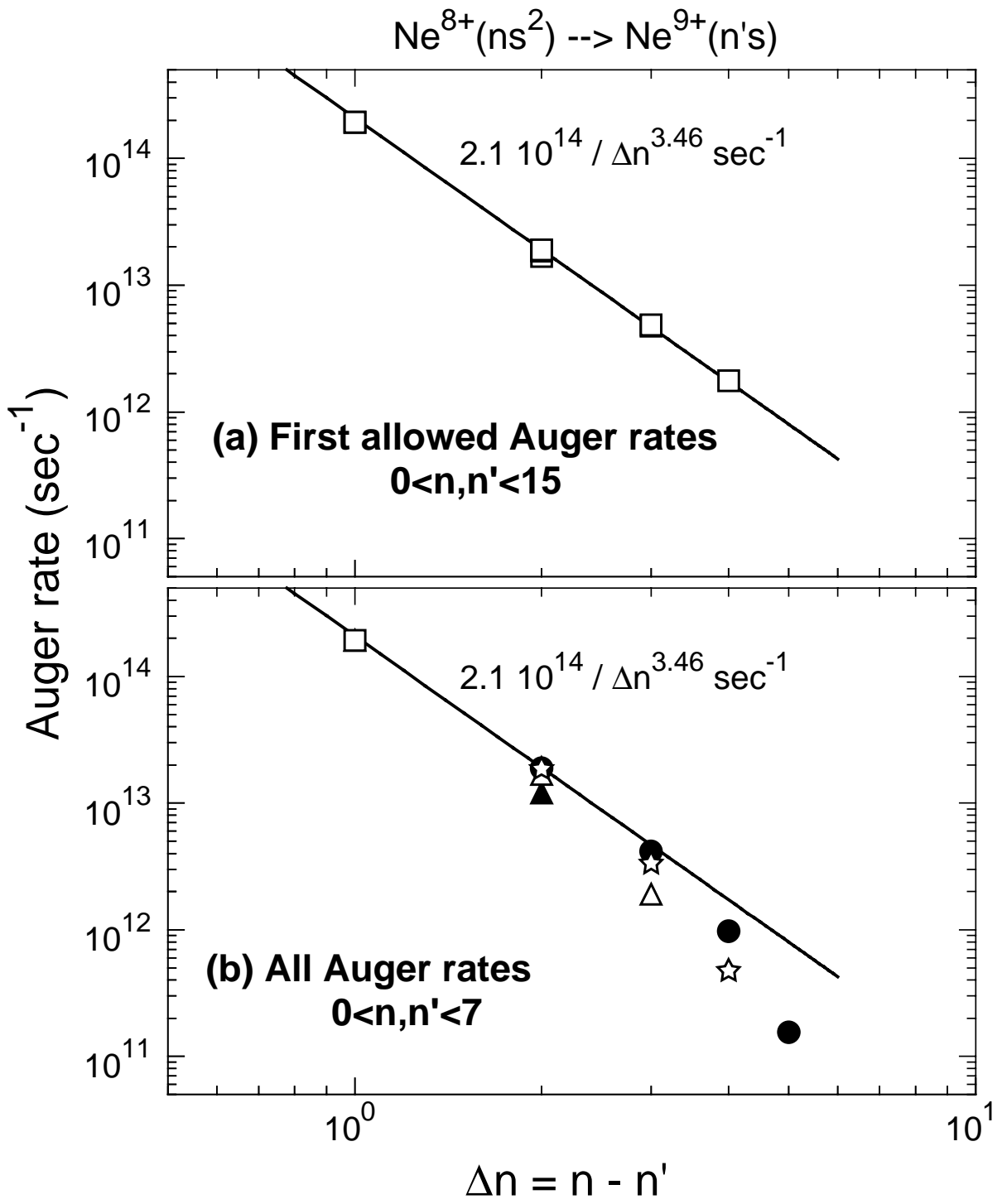


Figure 2

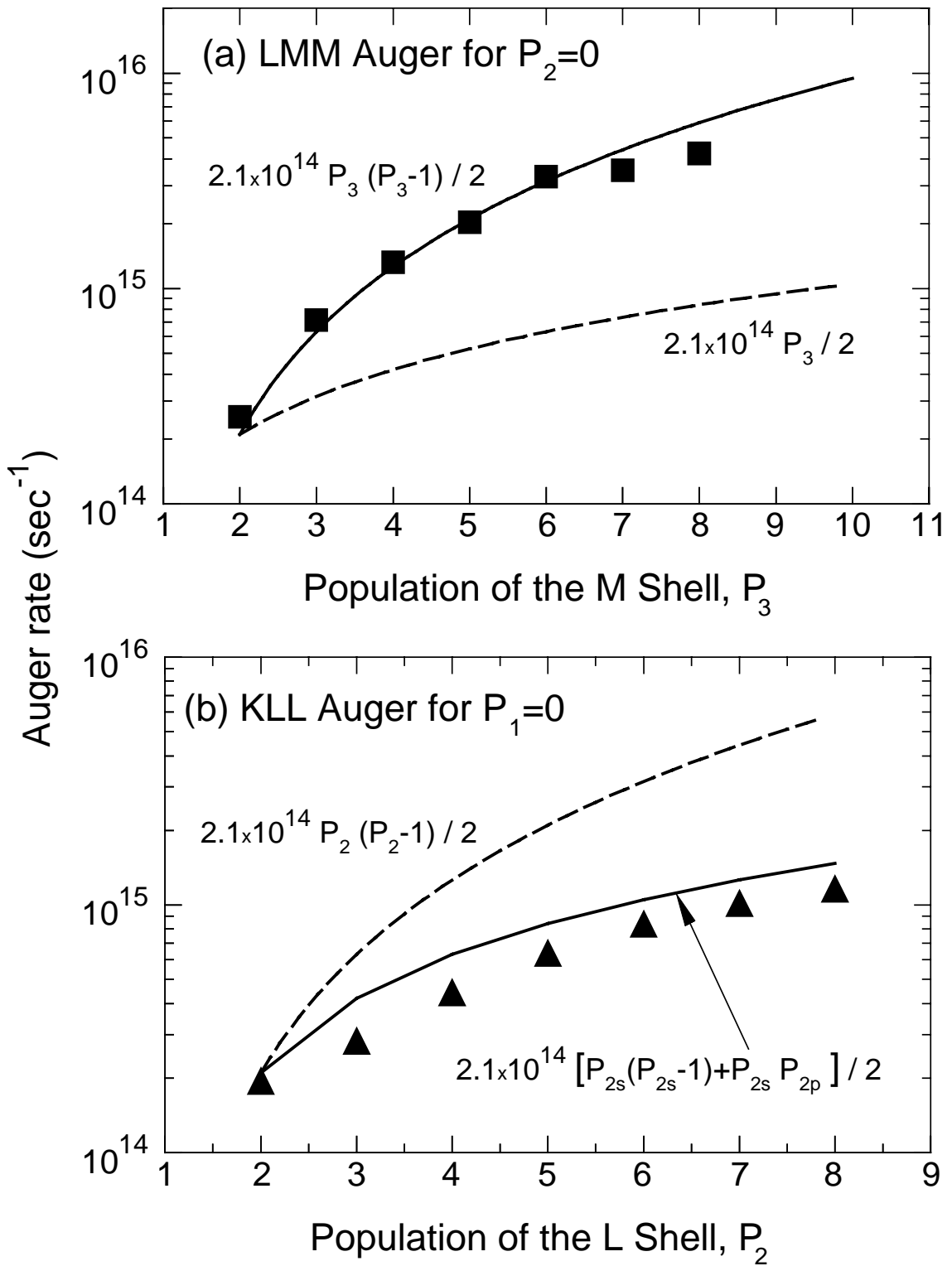


Figure 3

LMM Auger rate for $P_3=2$

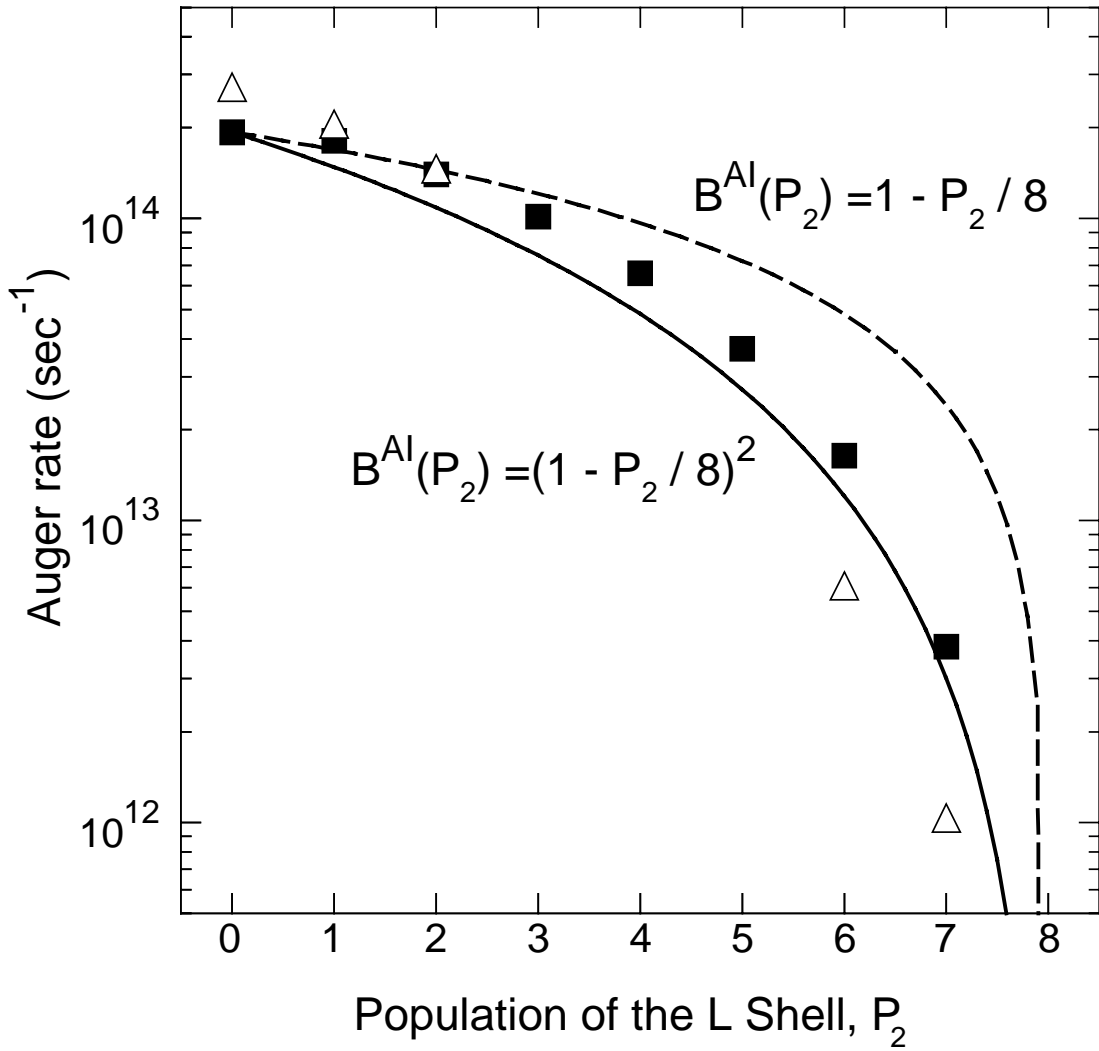


Figure 4

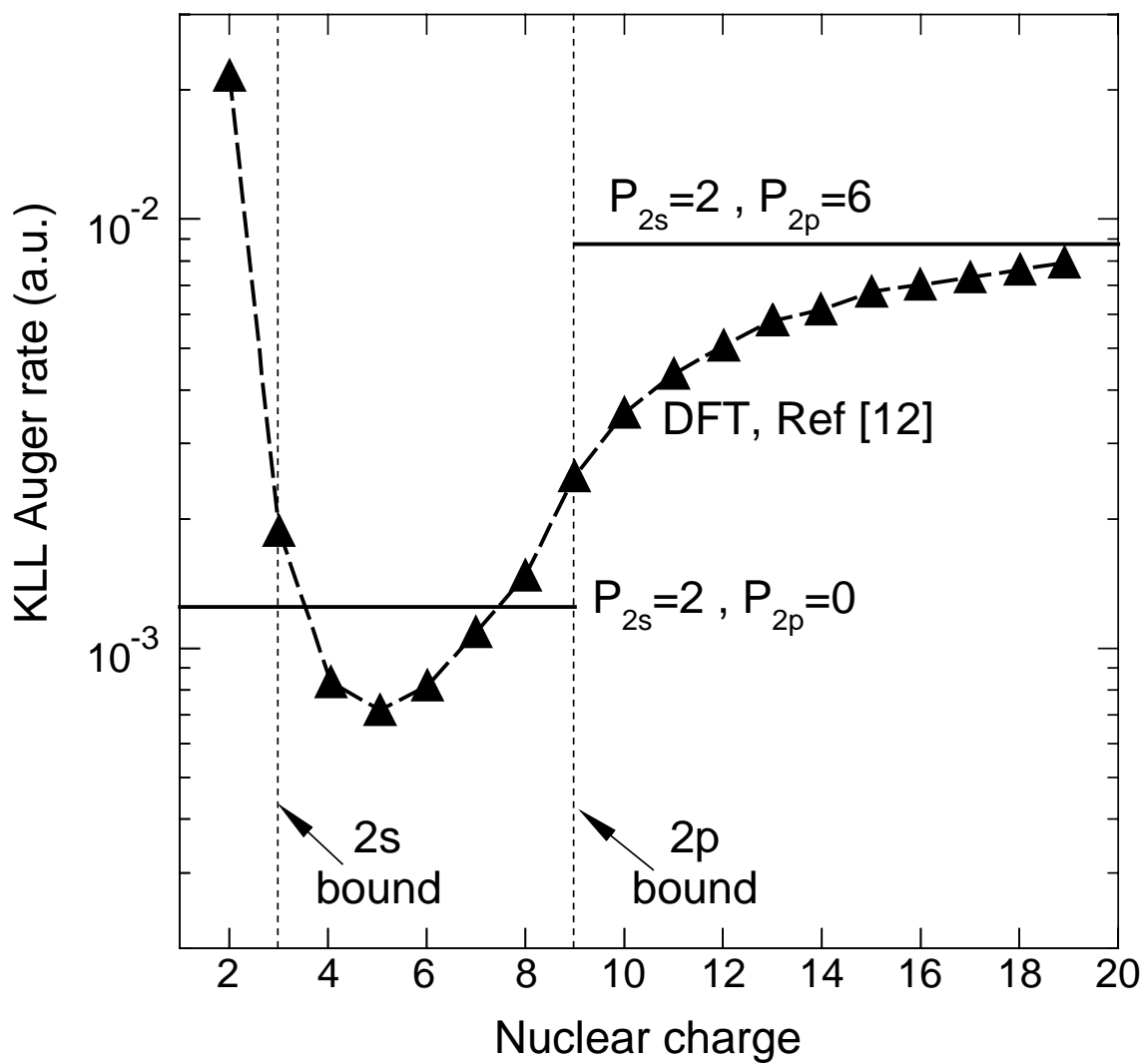


Figure 5

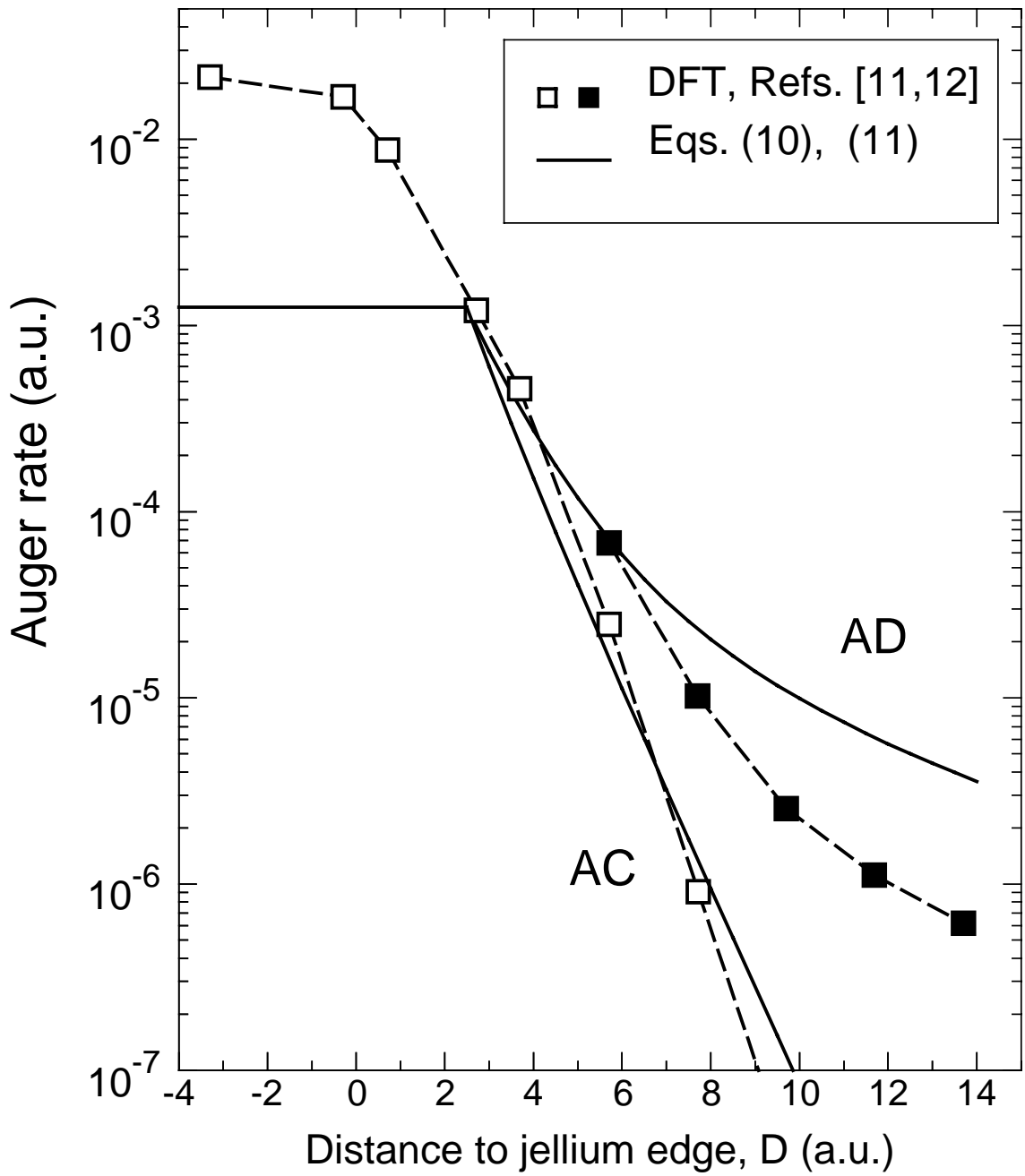


Figure 6